

Interfacial instabilities in confined displacements involving non-Newtonian fluids

Vaibhav Raj Singh Parmar^{1, †} and Ranjini Bandyopadhyay^{1, *}

¹*Soft Condensed Matter Group, Raman Research Institute, C. V. Raman Avenue, Sadashivanagar, Bangalore 560 080, INDIA*

November 20, 2023

Abstract

The growth of interfacial instabilities during fluid displacements can be driven by gradients in pressure, viscosity and surface tension, and by applying external fields. Since displacements of non-Newtonian fluids such as polymer solutions, colloidal and granular slurries are ubiquitous in natural and industrial processes, understanding the growth mechanisms and fully-developed morphologies of interfacial patterns involving non-Newtonian fluids is extremely important. In this perspective, we focus on displacement experiments wherein competitions between capillary, viscous, elastic and frictional forces drive the onset and growth of interfacial instabilities in confined geometries. We conclude by highlighting several exciting open problems in this research area.

1 Introduction

Ideal solids like metals follow Hooke's law, while ideal fluids like air, water and small-molecule oils satisfy Newton's law of viscosity. In contrast, non-Newtonian fluids such as blood, saliva, lava, colloidal clay suspensions, polymers and food are composed of weakly-interacting macromolecules and can simultaneously exhibit shear rate dependent viscous and elastic responses [1]. This class of materials, ubiquitous in our day-to-day lives and in industrial, therapeutic and geophysical processes, is easily deformed by thermal stresses and often referred to as 'soft matter'.

[†]vaibhav@rri.res.in

^{*}Corresponding Author: Ranjini Bandyopadhyay; Email: ranjini@rri.res.in

The particle-particle and particle-solvent interactions in colloidal suspensions [1] can lead to the formation of fragile, heterogeneous microstructures. Soft materials have non-zero relaxation times and display shear-dependent flow and deformation properties (rheology) [2]. The sample viscosity can decrease with shear due to rupture of the underlying microstructures in a shear-thinning process [3]. Aqueous suspensions of charged colloidal clays display time-dependent mechanical properties due to a gradual and spontaneous evolution of inter-particle interactions in a physical aging process [4]. Viscoplastic materials with non-zero yield stresses σ_y [5] are composed of microstructures that resist flow at small deformations, but exhibit liquid-like response at stresses exceeding σ_y . The viscoelasticity of polymeric fluids arises from entanglements between neighbouring polymers that provide an effective elastic force, thereby offering enhanced resistance to flow. Dense granular suspensions such as sand-water slurries and concrete, comprising non-Brownian particles suspended in a viscous fluid, can also exhibit viscoplastic flow [6]. Some non-Newtonian granular materials such as cornstarch suspensions display non-monotonic flow curves (stress *vs.* strain rate plots), with shear-thinning rheology preceding shear-thickening behaviour (increase in viscosity with shear rate due to buildup of microstructure) [6]. Notable among the models to describe the gamut of viscoelastic flows (Fig. 1(a)) [2] is the power law model for shear-thinning and shear-thickening materials: $\eta(\dot{\gamma}) = K\dot{\gamma}^{n-1}$ [2], where $\eta(\dot{\gamma})$ is the shear rate ($\dot{\gamma}$) dependent viscosity of the fluid, K is the flow consistency index and n is a power law index. This model describes shear-thinning and shear-thickening respectively for $n < 1$ and $n > 1$. Other models for more realistic non-Newtonian fluids [2] include the Cross, Carreau-Yasuda, upper convected Maxwell (UCM) and Oldroyd-B models for shear-thinning materials and the Hershel-Bulkley model for yield-stress fluids.

Multiphase flows in porous media are important in membrane separation, sanitation systems, drying and enhanced mixing processes, and also for enhanced oil recovery, sugar refining and carbon sequestration [11–16]. The interfacial velocity u of a Newtonian fluid with viscosity η in a porous medium of permeability κ is described by Darcy’s law [12], $u = -\frac{\kappa}{\eta}\nabla P$, where P is the pressure field. An interfacial instability characterised by the emergence of viscous fingers [13, 17–19] results when a fluid of lower viscosity η_{in} displaces another one of higher viscosity η_{out} in a medium of permeability κ . Wetting-induced flows, such as invasion percolation, cooperative pore filling, and corner flows were reported in capillary-dominated displacement experiment [20]. Interestingly, depending on the viscosity contrast of the fluid pair, both unstable and stable flows were seen in viscosity-dominated displacement experiments [17]. The growth of viscous fingers *via* successive tip-splitting results in intricate interfacial

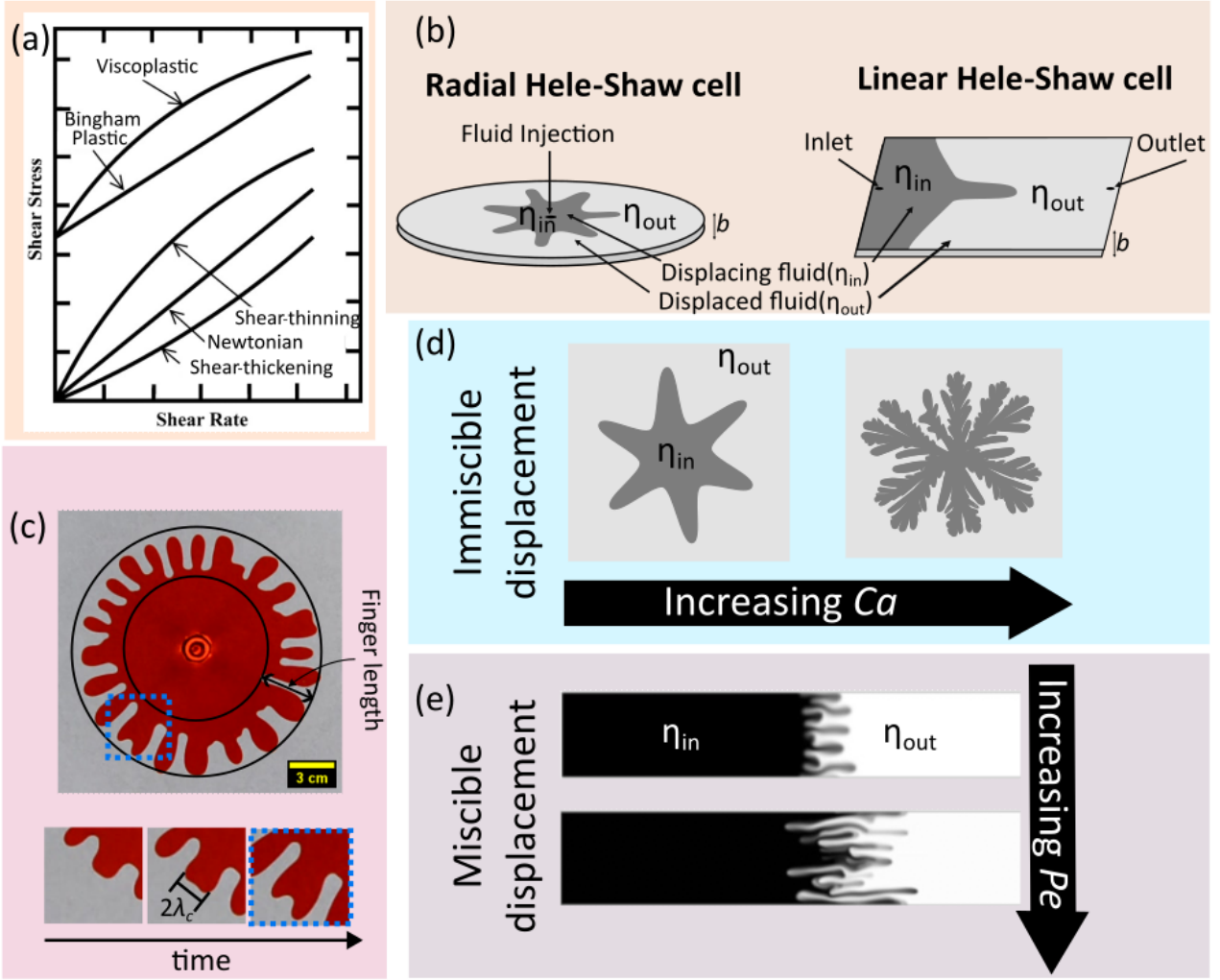


Fig. 1: **Non-Newtonian flows, experimental setups and the viscous fingering instability.** (a) Classification of non-Newtonian fluids based on flow curves. (b) Schematic diagrams of radial and linear Hele-Shaw (HS) cells. (c) The length and width, λ_c , of a viscous finger. Formation of complex interfacial instabilities with increasing (d) capillary number Ca and (e) Peclet number Pe . (a,c,d) are adapted from [7–9] and (e) is reproduced with permission from [10].

patterns that have been investigated in radial and linear Hele-Shaw (HS) cell geometries (Fig. 1(b)). Flow in a HS cell, comprising a pair of transparent plates separated by an infinitesimally small gap b [19], is mathematically equivalent to that in a porous medium and can be described by Darcy’s Law, with $\kappa = b^2/12$ [17].

A growing finger is completely described by its width and length (Fig. 1(c)). The finger width, which depends on the competition between destabilising viscous forces [17] and stabilising capillary forces [18], is characterised by the most unstable wavelength, $\lambda_c = \pi b \sqrt{\frac{1}{Ca}}$, where $Ca = \frac{\Delta\eta u}{\gamma}$ is the ratio of viscous and capillary forces, $\Delta\eta$ is the viscosity contrast of the two fluids and γ is the interfacial

tension [13]. The onset of instability and length of the propagating finger in a radial HS cell [21, 22] are set by the viscosity ratio of the fluid pair, η_{in}/η_{out} . Experimentally observed finger widths were seen to deviate from the classical prediction [17] at high capillary numbers Ca [23, 24]. In miscible displacements ($\gamma \approx 0$ and high Ca), there is no well-defined interface between the displacing and displaced fluids due to diffusion-driven interfacial mixing [25]. In such cases, interfacial instabilities depend on the ratio of advective and diffusive timescales, the Peclet number $Pe = uL/D$, with L being the lengthscale characterising the system and D its diffusion coefficient [13, 26]. The intricate and complex interfacial patterns that form at high Ca in immiscible displacements and at high Pe in miscible cases are shown in Figs. 1(d) and (e) respectively. For confined displacements involving at least one non-Newtonian fluid with a relaxation time τ_r , the growth and development of interfacial patterns are significantly different when compared to experiments involving Newtonian fluids, and additional dimensionless numbers [27] such as Deborah number, $De = \tau_r/T$, and Weissenberg number, $Wi = 2\tau_r\dot{\gamma}$, determine interfacial growth. Here, T is the characteristic time of the deformation process and $\dot{\gamma} = 2U/b$ [28] is the characteristic deformation/shear rate.

In this perspective, we review the development of interfacial instabilities in displacement processes involving non-Newtonian fluids in Hele Shaw cells. We focus on scenarios driven by competitions between viscous, capillary, elastic and frictional forces, wherein the contributions of gravity and inertia are negligible. We discuss recent progress in the study of morphologies and growth mechanisms of interfacial patterns and conclude by highlighting open questions in this research area.

2 Role of shear-thinning on interfacial instability

Linder *et.al.* [29] displaced shear-thinning solutions of the stiff polymer Xanthan by heptane oil. For low polymer concentrations, the finger width satisfies the classical prediction for two-dimensional potential flow for Newtonian fluids [30], but with the shear rate dependence of the viscosity, $\eta(\dot{\gamma}) = \eta_{eff}$, taken into account in a modified Darcy's law (Fig. 2(a)). Finger narrowing and deviation from classical predictions were noted with increasing polymer concentration. Due to thinning of the displaced fluid under large driving pressures, the velocity of the propagating finger is maximum at the tip. The resistance to finger growth is therefore minimum in the forward direction [31], which results in the emergence of increasingly pointed fingers [32]. The pressure field, which is Laplacian ($\nabla^2 P = 0$) for Newtonian fluids, becomes non-Laplacian ($\nabla \left[|\nabla P|^{\frac{1}{n}-1} \nabla P \right] = 0$) when strongly shear-thinning

materials are displaced and is described by a generalised Darcy’s law [31]:

$$u = - \left[\frac{n}{(2n + 1)K^{\frac{1}{n}}} \left(\frac{b}{2} \right)^{\frac{1}{n}+1} \right] |\nabla P|^{\frac{1}{n}-1} \nabla P \quad (1)$$

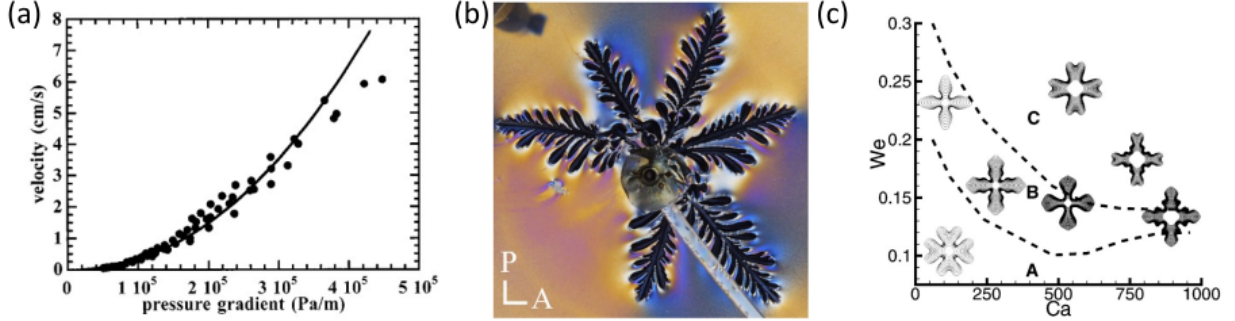


Fig. 2: **Effect of shear-thinning on viscous fingering.** (a) Finger velocity *vs.* pressure gradient during displacement of shear-thinning fluids. Strongly shear-thinning fluids deviate from the prediction of Darcy’s law (solid line). (b) Dendritic patterns *via* repeated side-branching in immiscible displacement of a shear-thinning nematic liquid crystal. (c) Effects of Weissenberg and capillary numbers on interfacial patterns due to immiscible displacement of a strongly shear-thinning polymeric fluid by air. Reproduced with permission from [33–35].

Simulations [35, 36] of displacements of weakly shear-thinning fluids using generalised Darcy’s law showed delayed onset of tip-splitting and the formation of narrow fingers. In contrast, tip splitting was completely suppressed in strongly shear-thinning fluids. Finger-narrowing, driven by shear-thinning of the displaced fluid, competes with finger-broadening under large driving pressures. Finger-tip oscillations, substantial side branching and dendritic pattern formation (Fig. 2(b)) were observed when a lyotropic chromonic liquid crystal was displaced by low-viscosity silicone oil in a radial HS cell [34]. A morphological phase diagram for displacement of a strongly shear-thinning fluid is reproduced in Fig. 2(c). Nonlinear mode coupling theory [31] and linear perturbation analysis [37] predict the emergence of side branches during displacement of shear thinning fluids. A transition from tip-splitting to side branching growth regimes was seen with decreasing n ($0.76 < n < 1.0$) and increasing De [38]. Experimental studies involving carbopol solutions, clay suspensions, liquid crystals, polymer solutions [34, 39–45] and numerical simulations using Oldroyd-B fluids [46] have reported the formation of side branches and dendrites.

In results that are reminiscent of those reported in experiments involving a Newtonian fluid pair [21, 22, 47], proportionate pattern growth and suppression of the fingering instability were reported when shear-thinning granular cornstarch suspensions were displaced by glycerol-water mixtures of controlled viscosity ratios, $0.06 < \eta_{in}/\eta_{out} < 0.95$ [48]. Interestingly, unstable to stable growth was observed when an aqueous shear-thinning Xanthan gum solution was displaced by mineral oil at $\eta_{in}/\eta_{out} > 1$ [49]. Finite volume simulations of the displacement of a more viscous Newtonian fluid by a shear-thinning fluid showed instability enhancement and finger coalescence [50]. Linear stability analysis and nonlinear simulations revealed flow stabilisation in anisotropic porous media when permeability and dispersion along the direction of flow was greater than along the transverse direction [51]. Interestingly, when a shear-thinning fluid was injected/withdrawn through millimetre-sized apertures at appropriately high flow rates, radial growth of thin equispaced protrusions (fringes) and enhanced fluid mixing were reported [47]. These observations were unaffected by turbulence, diffusion, elongation and elastic effects. The physical principles governing such pattern formation remain elusive.

3 Role of elasticity and yield stress on interfacial instability

Shear-induced rupture of the underlying microscopic structures constituting an elastic fluid results in a reduction of sample viscosity. Distinguishing the specific roles of elasticity and shear-thinning while describing the flows of elastic fluids is therefore challenging. The exact effect of sample elasticity on material flow can be isolated using Boger fluids [52], which are elastic fluids with constant viscosities comprising dilute polymers in highly viscous solvents. Large normal stresses are generated at the tip of a propagating finger during displacement of an elastic fluid. When compared to a Newtonian fluid displacement experiment, tip-splitting events occurred at lower injection pressures when a Boger fluid was displaced by immiscible air in a linear HS cell [53]. While miscible displacement of a Newtonian fluid in a linear geometry gives rise to a single dominant finger, displacement of a Boger fluid under identical conditions results in many narrow, long fingers with reduced shielding (Fig. 3(a,b)) [54]. The localised hardened zones that form at the fingertips due to very high normal stresses result in inhibited finger growth and interaction, as shown in simulations of displacement experiments involving elastic fluids with $0.005 < Wi < 5$ [55]. Interestingly, replacing one the HS plates with an elastic membrane resulted in suppression of viscous fingering during displacement of a Newtonian fluid [56]. In these experiments, membrane deformation in response to fluid flow generates a restoring force that opposes

viscous destabilisation.

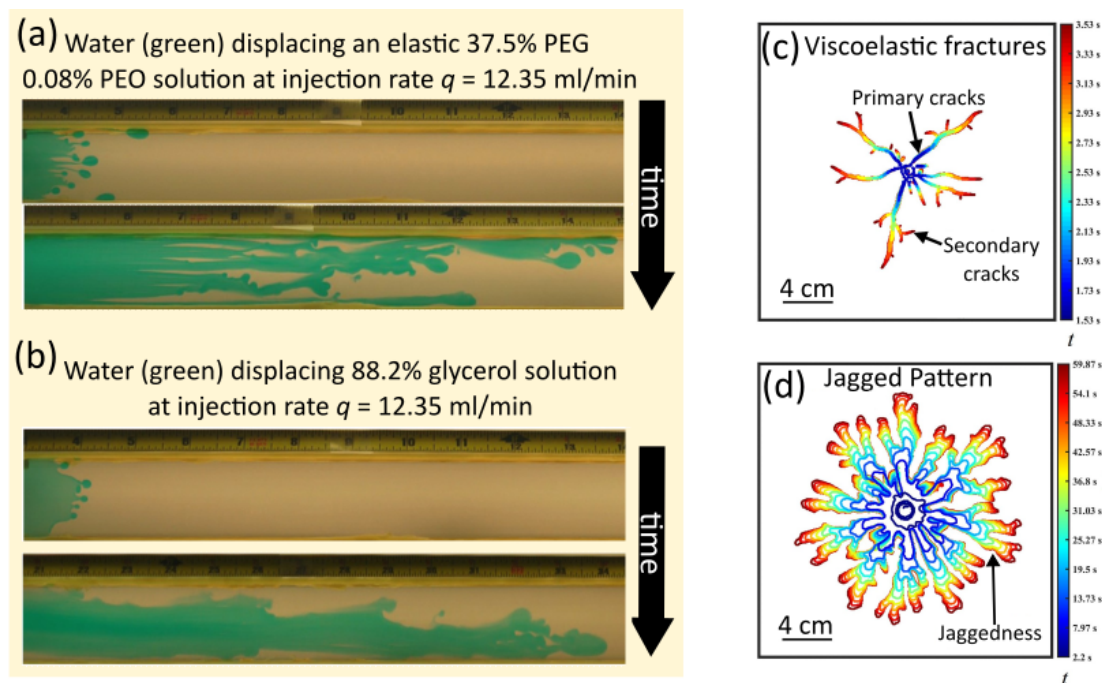


Fig. 3: **Effect of elasticity on viscous fingering.** Distinct finger morphologies during displacements of (a) an elastic fluid and (b) a Newtonian fluid in a linear HS cell. (c) Viscoelastic fractures (VEF) formed by displacing an elastic aqueous clay suspension by miscible water. (d) Jagged interfacial pattern during displacement of the elastic clay suspension by immiscible oil. Reproduced with permission from [42, 54].

Viscoelastic fluids behave as elastic solids at $De \gg 1$. An aqueous suspension of clay spontaneously transitions from a liquid to a soft solid-like phase with increasing concentration and due to physical aging [4, 57]. In confined radial displacements of aqueous clay suspensions of increasing concentrations, a transition from viscous fingering (VF) to viscoelastic fracturing (VEF, Fig. 3(c)) was reported [58]. We note that the emergence of VEF, characterised by a small number of primary branches with perpendicular secondary offshoots, implies solid-like response of the displaced suspension. Miscible displacement of aqueous solutions of hydrophobic polyoxyethylene, an associating polymer solution, showed a transition from VF to VEF with increasing polymer concentration and injection pressure [59]. However, a VF-VEF transition was not observed in an entangled homopolymer solution, demonstrating the importance of associating networks in fracture formation. During the immiscible displacement of a self-assembled transient gel, a fingering regime was reported at low injection pressures, wherein the gel was displaced gently and long range flows were generated [60]. At higher injection pressures, the gel exhibited a solid-like response and was torn apart by the displacing fluid, resulting in fracture formation

and absence of long-range flows. A dimensionless parameter $\tilde{\lambda} = \frac{b^2(-\nabla P)^{3/2}}{G\gamma^{1/2}}$ [61] was introduced to characterise the VF-VEF transition for an upper convected Maxwell fluid [62] of shear modulus G . While VF was observed for small values of $\tilde{\lambda}$, the finger growth rate diverged above a critical $\tilde{\lambda}$ due to onset of fracturing.

When displaced at stresses below their yielding thresholds σ_y [39, 63, 64], the solid-like/ elastic response of yield stress fluids resulted in the formation of jagged patterns and asymmetric fingers [65]. A ramified interface developed by the repeated tip-splitting of asymmetric fingers during the immiscible displacement of elastic carbopol solutions with air in a linear HS cell [65]. In such displacement experiments, the width of the finger is set by $\sqrt{\gamma b/\sigma_y}$ and flows become increasingly unstable with increasing roughness of the HS cell plate [66, 67]. Since the low interfacial tension in a miscible displacement experiment reduces fracture energy, viscoelastic fractures (VEF) are more likely to form in miscible rather than in immiscible displacements of yield stress fluids below their yielding points [68]. A transition from VEF to pattern growth driven by fingertip splitting was reported when a miscible displacing fluid was injected at a rate that resulted in yielding of an emulsion [69]. When elastic foam was displaced by air at increasing driving pressures, jagged interfacial patterns (Fig. 3(d)) observed below the yielding point transitioned to smooth fingers (Fig. 1(c)) in the viscosity-dominated regime [70]. When aqueous clay suspensions of increasing ages were radially displaced by miscible water at low injection rates, a sequence of interfacial patterns, from dense viscous to dendrites and eventually VEFs, were observed [41, 42]. In contrast, when the aging suspensions were displaced by immiscible mineral oil, a transition from flower (Fig. 1(c)) to jagged (Fig. 3(d)) patterns was observed.

4 Role of shear-thickening on interfacial instability

Displacement of a shear-thickening fluid produces wide fingers that grow *via* rapid tip-splitting events [31, 71, 72]. For strongly shear-thickening fluids, finger propagation slows down substantially to a value below the prediction of the modified Darcy’s law (Fig. 4(a), [69]).

Shear-thickening fluids display continuous shear-thickening (CST), discontinuous shear-thickening (DST), and shear-jamming (SJ) flow regimes with increasing particle volume fraction ϕ and applied shear stress σ / rate $\dot{\gamma}$ [6]. These distinct rheological regimes of cornstarch suspensions can be achieved in radial displacements experiments by appropriately controlling the injection pressures of the displacing Newtonian fluids [74–76]. When cornstarch suspensions in CST, DST and SJ were displaced by

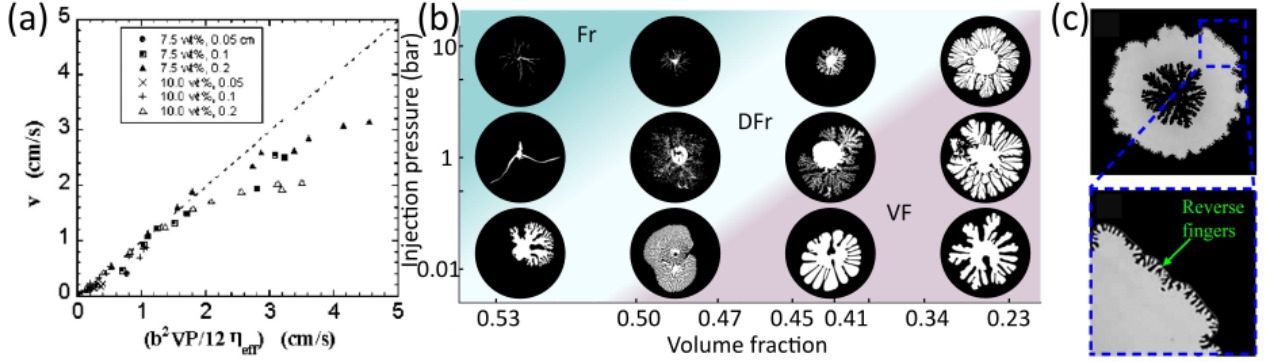


Fig. 4: **Effect of shear-thickening on interfacial instability.** (a) Average finger velocity as a function of $b^2 \nabla P / 12 \eta_{eff}$ [73]. Strongly shear-thickening fluids show substantial deviations from Darcy’s law (dashed line). (b) Phase diagram in the pressure-volume fraction plane displaying viscous fingers (VF), dendritic fractures (DFr) and large-scale fracturing (Fr). (c) Formation of reverse fingers due to invasion of air at the outermost interface between a discontinuously shear-thickening cornstarch suspension and atmospheric air. Reproduced with permission from [73–75].

immiscible air in separate experiments, three distinct interfacial patterns, *viz.*, viscous fingers (VF), dendritic fracturing (DFr) and system-wide fracturing (Fr)(Fig. 4(b)) were produced [74]. A transition from VF to VEF was reported in cornstarch suspensions when oil was used as a displacing fluid [76]. Miscible displacements of discontinuously shear thickening cornstarch suspensions with water [75] showed transient invasion of air into the suspension and formation of reverse fingers at the outermost interface between the suspension and atmospheric air (Fig. 4(c)). Since the suspension was in the DST regime, the stresses due to injection of the displacing fluid are expected to propagate through force networks. Suspension dilation [6], followed by a surface tension driven restoring force, drives the formation of the observed reverse fingers. To the best of our knowledge, there are no complete theoretical or numerical descriptions of dendritic fracturing and reverse finger formation in Hele-Shaw flows.

5 Interfacial instabilities in multiphase frictional and viscous flows

In this section, we focus on displacement processes involving movable athermal grains. Advancements in the understanding of multiphase flows in granular media have been summarised recently [16, 77]. For granular particles that move during displacement [16, 78–81], the inter-grain solid friction assumes a crucial role in understanding their flow [82]. At low grain fraction ϕ , the flow profile was reported to obey modified Darcy’s law, with grain sizes determining the lengthscale of the instability [83]. Polydisperse glass beads, suspended in a glycerol-water mixture and displaced by air, accumulated at the interface to

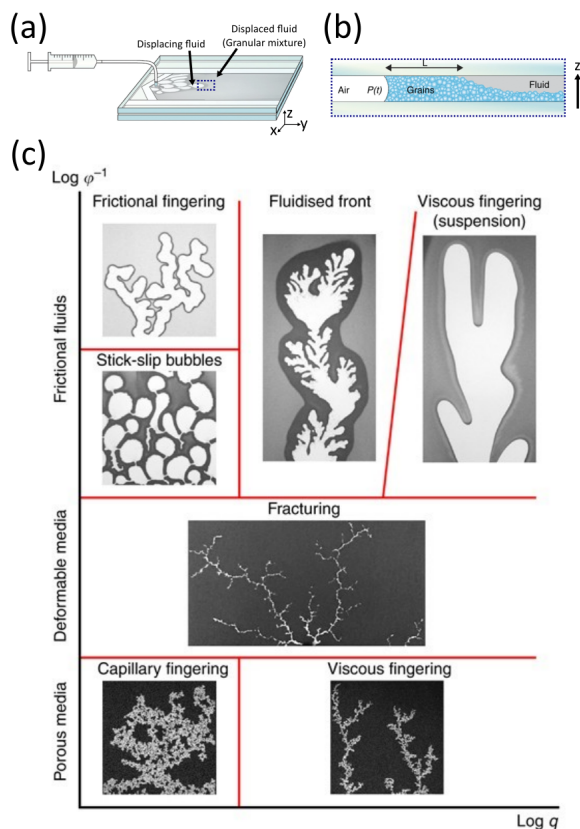


Fig. 5: **Pattern formation during displacement of deformable granular matter.** Schematic illustrations of (a) a rectilinear Hele-Shaw cell used for granular displacement experiments and (b) the formation of a compact front of grains due to the bulldozing effect. (c) Phase diagram in the inverse of volume fraction, ϕ^{-1} , and injection rate, q , plane, displaying various interfacial pattern morphologies during displacement of deformable granular media undergoing drainage. Reproduced with permission from [78].

form a compact front (contact angle $\theta > 90^\circ$, experimental geometry reproduced in Fig. 5(a)) [78]. This phenomenon, known as bulldozing, occurs when the threshold capillary pressure exceeds inter-grain frictional resistance to sliding and rearrangements, and is displayed in Fig. 5(b). Friction-dominated finger dynamics was reported at low injection rates, and a transition from a creeping fingering process to intermittent stick-slip bubble dynamics was seen with increasing ϕ (Fig. 5(c)). As the viscous forces become significant with increasing injection rates, fluidisation of the compact granular front and viscous fingering were reported [78,82]. Bulldozing causes frictional instability in the flow at all injection rates, however, viscous forces can stabilise the flow if $\eta_{in} > \eta_{out}$. A study investigated the competition between stabilising viscous forces and destabilising frictional forces by injecting glycerol-water mixture into dry hydrophobic grains [84]. A transition from frictional fingers to stable displacement with radial spikes of grains was reported with increasing injection pressure, η_{in} and volume fraction inverse, ϕ^{-1} .

The response of the displaced medium changed from fluid-like to solid-like at high ϕ , with the emergence of fractures at high injection pressures. These results are depicted in Fig. 5(c).

When spherical glass beads were displaced by air in a radial HS cell in the zero surface tension limit ($\theta \approx 0^\circ$), very sharp fingers grew via successive tip splitting when the injection pressure exceeded the suspension yield stress [85]. In contrast to Newtonian fluid displacement, the fully developed pattern took on a highly ramified structure, but became smoother with wider fingers at higher injection pressures. Unlike Newtonian displacement patterns [86], the characteristic finger width in granular fingering is independent of the HS cell gap [85]. The bulldozing effect and frictional fingers were absent in this study [85] due to the negligible threshold capillary pressure. The observed differences between displacements of granular fluids and Newtonian fluids arise from the distinct dissipation mechanisms, frictional *vs.* viscous, in the two processes.

6 Summary and open questions

In this perspective, we have focussed on the distinct morphologies and growth mechanisms of interfacial patterns that result during the displacement of non-Newtonian colloidal and granular fluids in radial and linear Hele-Shaw cells. These studies clearly demonstrate the important role of fluid rheology in pattern formation. There are many other experimental setups used to study fluid-fluid displacements [87] that we have not discussed due to space constraints. We would like to refer the reader to the literature involving lifting Hele-Shaw cells, wherein the cell gap is time-dependent [88,89] and inertial effects influence the growth of the emergent interfacial patterns [90]. Injecting the displacing fluid at a non-uniform rate can suppress the viscous fingering instability for both Newtonian and non-Newtonian displacements [91,92]. Tapered Hele-Shaw cells, with cell plates that are not parallel, have been reported to reduce the viscous fingering instability [93]. A multiport lifted Hele-Shaw cell with multiple source holes has been used to engineer complex interlinked meshes [94], while experiments with rotating Hele-Shaw cells have been performed to study density-driven instabilities [95]. Displacement experiments involving a pair of chemically reactive fluids in a Hele-Shaw cell have reported dramatic changes in the morphology and growth of viscous fingers [14]. Electro-osmotic flows have been induced by applying electric fields to control viscous fingers in Newtonian [96] and non-Newtonian fluid displacements [97]. Among other cell configurations not discussed in this perspective are fluid withdrawal experiments, wherein viscous and particle-driven instabilities have been reported [98,99].

While the role of material shear rheology has been the main focus in studies of the viscous fingering instability, exploiting the extensional rheology of non-Newtonian fluids holds a lot of promise in our ability to control fluid displacement processes [53,100]. The effect of interfacial flows in the presence of surface active agents [101] is an area that also remains relatively less explored for non-Newtonian fluid displacements. Local events in viscous fingering [13,53] are comparatively better studied than for viscoelastic fracture formation. Analytical and numerical investigations are essential for acquiring fundamental knowledge of elasticity-driven interfacial instabilities. Appropriate models need to be developed to explain other novel phenomena that have been observed in experiments, for example, the formation of fringes [47], asymmetric [65] and reverse fingers [75], and dendritic fractures [74]. Many non-Newtonian fluids show chaotic flows at low Reynolds numbers and are known to generate anomalous flow resistance [102]. The formation of viscous fingers can expedite fluid mixing at low Reynolds numbers [103]. Detailed studies on how chaotic flows affect the viscous fingering instability and fluid mixing are therefore critical. Tuning interactions between the macromolecular constituents of non-Newtonian fluids modifies fluid rheology [104] and can be exploited to pre-program interfacial instability patterns. The ability to control, enhance and suppress finger formation, and therefore fluid displacement efficiency [46], is crucial in several industrial processes, calling for further rigorous study of the mechanisms of formation of complex interfacial instability patterns.

Data Availability

No new data were created or analysed in this article.

Acknowledgments

The authors thank Raman Research Institute, Bangalore, India, for financial support.

References

- [1] H. W. D. Fennell Evans, *The Colloidal Domain: Where Physics, Chemistry, Biology, and Technology Meet*, 2nd Edition, Wiley-VCH, 1999.
- [2] C. W. Macosko, *Rheology: Principles, Measurements and Applications*, Wiley-VCH, 1994.

- [3] E. Dickinson, Basic principles of colloid science: By D. H. Everett, Royal Society of Chemistry, London, 1988., *J. Chem. Technol. Biotechnol.* 45 (4) (1989) 328–329. doi:10.1002/jctb.280450412.
- [4] H. Van Olphen, *An Introduction to Clay Colloid Chemistry: For Clay Technologists, Geologists and Soil Scientists*. 2nd edition, Wiley, New York, 1977.
- [5] P. Coussot, Yield stress fluid flows: A review of experimental data, *J. Non-Newton. Fluid Mech.* 211 (2014) 31–49. doi:https://doi.org/10.1016/j.jnnfm.2014.05.006.
- [6] J. F. Morris, Shear Thickening of Concentrated Suspensions: Recent Developments and Relation to Other Phenomena, *Annu. Rev. Fluid Mech.* 52 (1) (2020) 121–144. doi:10.1146/annurev-fluid-010816-060128.
- [7] R. P. Chhabra, *Non-Newtonian Fluids: An Introduction*, Springer New York, New York, NY, 2010, Ch. 1, pp. 3–34. doi:https://doi.org/10.1007/978-1-4419-6494-6.
- [8] I. Bischofberger, R. Ramachandran, S. R. Nagel, An island of stability in a sea of fingers: emergent global features of the viscous-flow instability, *Soft Matter* 11 (2015) 7428–7432. doi:10.1039/C5SM00943J.
- [9] J.-D. Chen, Growth of radial viscous fingers in a hele-shaw cell, *J. Fluid Mech.* 201 (1989) 223–242. doi:10.1017/S0022112089000911.
- [10] Y. F. Deki, Y. Nagatsu, M. Mishra, R. X. Suzuki, Numerical study of the effect of pécelet number on miscible viscous fingering with effective interfacial tension, *J. Fluid Mech.* 965 (2023) A22. doi:10.1017/jfm.2023.405.
- [11] N. J. Balmforth, R. V. Craster, *Geophysical Aspects of Non-Newtonian Fluid Mechanics*, Springer Berlin Heidelberg, Berlin, Heidelberg, 2001, Ch. 2, pp. 34–51. doi:https://doi.org/10.1007/3-540-45670-8_2.
- [12] P. M. Adler, *Multiphase Flow in Porous Media*, Springer Dordrecht, 2023. doi:10.1007/978-94-017-2372-5.
- [13] G. M. Homsy, Viscous Fingering in Porous Media, *Annu. Rev. Fluid Mech.* 19 (1) (1987) 271–311. doi:10.1146/annurev.fl.19.010187.001415.

- [14] A. De Wit, Chemo-Hydrodynamic Patterns and Instabilities, *Annu. Rev. Fluid Mech.* 52 (1) (2020) 531–555. doi:10.1146/annurev-fluid-010719-060349.
- [15] A. Pinilla, M. Asuaje, N. Ratkovich, Experimental and computational advances on the study of Viscous Fingering: An umbrella review, *Heliyon* 7 (7) (2021) e07614. doi:https://doi.org/10.1016/j.heliyon.2021.e07614.
- [16] R. Juanes, Y. Meng, B. K. Primkulov, Multiphase flow and granular mechanics, *Phys. Rev. Fluids* 5 (2020) 110516. doi:10.1103/PhysRevFluids.5.110516.
- [17] P. G. Saffman, G. I. Taylor, The penetration of a fluid into a porous medium or Hele-Shaw cell containing a more viscous liquid, *Proc. R. Soc. A: Math. Phys. Eng. Sci.* 245 (1242) (1958) 312–329.
- [18] J.-D. Chen, Radial viscous fingering patterns in Hele-Shaw cells, *Exp. Fluids* 5 (6) (1987) 363–371.
- [19] L. Paterson, Radial fingering in a Hele Shaw cell, *J. Fluid Mech.* 113 (1981) 513–529.
- [20] B. K. Primkulov, A. A. Pahlavan, X. Fu, B. Zhao, C. W. MacMinn, R. Juanes, Wettability and Lenormand’s diagram, *J. Fluid Mech.* 923 (2021) A34. doi:10.1017/jfm.2021.579.
- [21] I. Bischofberger, R. Ramachandran, S. R. Nagel, Fingering versus stability in the limit of zero interfacial tension, *Nat. Commun.* 5 (1) (2014) 5265.
- [22] E. Lajeunesse, J. Martin, N. Rakotomalala, D. Salin, 3D Instability of Miscible Displacements in a Hele-Shaw Cell, *Phys. Rev. Lett.* 79 (1997) 5254–5257. doi:10.1103/PhysRevLett.79.5254.
- [23] E. O. Dias, J. A. Miranda, Wavelength selection in Hele-Shaw flows: A maximum-amplitude criterion, *Phys. Rev. E* 88 (2013) 013016. doi:10.1103/PhysRevE.88.013016.
- [24] H. Kim, T. Funada, D. D. Joseph, G. M. Homsy, Viscous potential flow analysis of radial fingering in a Hele-Shaw cell, *Phys. Fluids* 21 (7) (2009) 074106. doi:10.1063/1.3184574.
- [25] S. Pramanik, M. Mishra, Effect of Péclet number on miscible rectilinear displacement in a Hele-Shaw cell, *Phys. Rev. E* 91 (2015) 033006. doi:10.1103/PhysRevE.91.033006.
- [26] V. Sharma, S. Nand, S. Pramanik, C.-Y. Chen, M. Mishra, Control of radial miscible viscous fingering, *J. Fluid Mech.* 884 (2020) A16. doi:10.1017/jfm.2019.932.

- [27] S. S. e. a. Datta, Perspectives on viscoelastic flow instabilities and elastic turbulence, *Phys. Rev. Fluids* 7 (2022) 080701. doi:10.1103/PhysRevFluids.7.080701.
- [28] R. Poole, The Deborah and Weissenberg Numbers, *Rheol. Bull. Br. Soc. Rheol.* 53 (2012) 32–39.
- [29] A. Lindner, D. Bonn, J. Meunier, Viscous fingering in complex fluids, *J. Condens. Matter Phys.* 12 (8A) (2000) A477. doi:10.1088/0953-8984/12/8A/366.
- [30] J. W. McLean, P. G. Saffman, The effect of surface tension on the shape of fingers in a Hele Shaw cell, *J. Fluid Mech.* 102 (1981) 455–469. doi:10.1017/S0022112081002735.
- [31] R. Brandão, J. a. V. Fontana, J. A. Miranda, Interfacial pattern formation in confined power-law fluids, *Phys. Rev. E* 90 (2014) 013013. doi:10.1103/PhysRevE.90.013013.
- [32] D. Bonn, H. Kellay, M. Bräunlich, M. Amar, J. Meunier, Viscous fingering in complex fluids, *Phys. A: Stat. Mech. Appl.* 220 (1) (1995) 60–73. doi:10.1016/0378-4371(95)00114-M.
- [33] A. Lindner, D. Bonn, J. Meunier, Viscous fingering in a shear-thinning fluid, *Phys. Fluids* 12 (2) (2000) 256–261. doi:10.1063/1.870303.
- [34] Q. Zhang, S. Zhou, R. Zhang, I. Bischofberger, Dendritic patterns from shear-enhanced anisotropy in nematic liquid crystals, *Sci. Adv.* 9 (2) (2023) eabq6820. doi:10.1126/sciadv.abq6820.
- [35] L. Kondic, M. J. Shelley, P. Palfy-Muhoray, Non-Newtonian Hele-Shaw Flow and the Saffman-Taylor Instability, *Phys. Rev. Lett.* 80 (1998) 1433–1436. doi:10.1103/PhysRevLett.80.1433.
- [36] P. Fast, L. Kondic, M. J. Shelley, P. Palfy-Muhoray, Pattern formation in non-Newtonian Hele-Shaw flow, *Physics of Fluids* 13 (5) (2001) 1191–1212. doi:10.1063/1.1359417.
- [37] P. Tordjeman, Saffman-Taylor instability of shear thinning fluids, *Phys. Fluids* 19 (11) (2007) 118102. doi:10.1063/1.2795213.
- [38] Y. H. Lee, J. Azaiez, I. D. Gates, Interfacial instabilities of immiscible non-Newtonian radial displacements in porous media, *Phys. Fluids* 31 (4) (2019) 043103. doi:10.1063/1.5090772.
- [39] A. Eslami, S. Taghavi, Viscous fingering regimes in elasto-visco-plastic fluids, *J. Non-Newton. Fluid Mech.* 243 (2017) 79–94. doi:https://doi.org/10.1016/j.jnnfm.2017.03.007.

- [40] H. Van Damme, F. Obrecht, P. Levitz, L. Gatineau, C. Laroche, Fractal viscous fingering in clay slurries, *Nature* 320 (6064) (1986) 731–733.
- [41] Palak, V. R. S. Parmar, D. Saha, R. Bandyopadhyay, Pattern selection in radial displacements of a confined aging viscoelastic fluid, *JCIS Open* 6 (2022) 100047. doi:10.1016/j.jciso.2022.100047.
- [42] Palak, V. R. S. Parmar, R. Bandyopadhyay, Growth kinetics of interfacial patterns formed by the radial displacement of an aging viscoelastic suspension, *JCIS Open* 10 (2023) 100084. doi:10.1016/j.jciso.2023.100084.
- [43] A. Buka, P. Palffy-Muhoray, Z. Rácz, Viscous fingering in liquid crystals, *Phys. Rev. A* 36 (1987) 3984–3989. doi:10.1103/PhysRevA.36.3984.
- [44] J. Nittmann, G. Daccord, H. E. Stanley, Fractal growth viscous fingers: quantitative characterization of a fluid instability phenomenon, *Nature* 314 (6007) (1985) 141–144.
- [45] P. Jangir, R. Mohan, P. Chokshi, Experimental study on the role of polymer addition in Saffman–Taylor instability in miscible flow displacement, *Phys. Fluids* 34 (9) (2022) 093102. doi:10.1063/5.0102237.
- [46] H. Shokri, M. H. Kayhani, M. Norouzi, Nonlinear simulation and linear stability analysis of viscous fingering instability of viscoelastic liquids, *Phys. Fluids* 29 (3) (2017) 033101. doi:10.1063/1.4977443.
- [47] N. Mehr, C. Roques, Y. Méheust, S. Rochefort, J. S. Selker, Mixing and finger morphologies in miscible non-Newtonian solution displacement, *Exp. Fluids* 61 (2020) 1–19.
- [48] Palak, R. Sathyanath, S. K. Kalpathy, R. Bandyopadhyay, Emergent patterns and stable interfaces during radial displacement of a viscoelastic fluid, *Colloids Surf. A: Physicochem. Eng. Asp.* 629 (2021) 127405. doi:https://doi.org/10.1016/j.colsurfa.2021.127405.
- [49] P. R. Vargas, P. E. Azevedo, B. S. Fonseca, P. R. de Souza Mendes, M. F. Naccache, A. L. Martins, Immiscible liquid-liquid displacement flows in a Hele-Shaw cell including shear thinning effects, *Phys. Fluids* 32 (1) (2020) 013105. doi:10.1063/1.5133054.

- [50] M. Norouzi, A. Yazdi, A. Birjandi, A numerical study on Saffman-Taylor instability of immiscible viscoelastic-Newtonian displacement in a Hele-Shaw cell, *J. Non-Newton. Fluid Mech.* 260 (2018) 109–119. doi:<https://doi.org/10.1016/j.jnnfm.2018.06.007>.
- [51] H. Shokri, M. Kayhani, M. Norouzi, Saffman–Taylor instability of viscoelastic fluids in anisotropic porous media, *Int. J. Mech. Sci.* 135 (2018) 1–13. doi:<https://doi.org/10.1016/j.ijmecsci.2017.11.008>.
- [52] D. F. James, Boger Fluids, *Annu. Rev. Fluid Mech.* 41 (1) (2009) 129–142. doi:[10.1146/annurev.fluid.010908.165125](https://doi.org/10.1146/annurev.fluid.010908.165125).
- [53] D. H. Vlad, J. V. Maher, Tip-splitting instabilities in the channel saffman-taylor flow of constant viscosity elastic fluids, *Phys. Rev. E* 61 (2000) 5439–5444. doi:[10.1103/PhysRevE.61.5439](https://doi.org/10.1103/PhysRevE.61.5439).
- [54] S. Malhotra, M. M. Sharma, Impact of fluid elasticity on miscible viscous fingering, *Chem. Eng. Sci.* 117 (2014) 125–135. doi:<https://doi.org/10.1016/j.ces.2014.06.023>.
- [55] P. Jangir, A. Herale, R. Mohan, P. Chokshi, Role of viscoelastic fluid rheology in miscible viscous fingering, *Int. J. Eng. Sci.* 179 (2022) 103733. doi:<https://doi.org/10.1016/j.ijengsci.2022.103733>.
- [56] D. Pihler-Puzović, P. Illien, M. Heil, A. Juel, Suppression of complex fingerlike patterns at the interface between air and a viscous fluid by elastic membranes, *Phys. Rev. Lett.* 108 7 (2012) 074502. doi:[10.1103/PHYSREVLETT.108.074502](https://doi.org/10.1103/PHYSREVLETT.108.074502).
- [57] D. Saha, R. Bandyopadhyay, Y. M. Joshi, Dynamic Light Scattering Study and DLVO Analysis of Physicochemical Interactions in Colloidal Suspensions of Charged Disks, *Langmuir* 31 (10) (2015) 3012–3020. doi:[10.1021/acs.langmuir.5b00291](https://doi.org/10.1021/acs.langmuir.5b00291).
- [58] E. Lemaire, P. Levitz, G. Daccord, H. Van Damme, From viscous fingering to viscoelastic fracturing in colloidal fluids, *Phys. Rev. Lett.* 67 (1991) 2009–2012. doi:[10.1103/PhysRevLett.67.2009](https://doi.org/10.1103/PhysRevLett.67.2009).
- [59] H. Zhao, J. V. Maher, Associating-polymer effects in a Hele-Shaw experiment, *Phys. Rev. E* 47 (1993) 4278–4283. doi:[10.1103/PhysRevE.47.4278](https://doi.org/10.1103/PhysRevE.47.4278).
- [60] G. Foyart, L. Ramos, S. Mora, C. Ligoure, The fingering to fracturing transition in a transient gel, *Soft Matter* 9 (2013) 7775–7779. doi:[10.1039/C3SM51320C](https://doi.org/10.1039/C3SM51320C).

- [61] S. Mora, M. Manna, Saffman-taylor instability of viscoelastic fluids: From viscous fingering to elastic fractures, *Phys. Rev. E* 81 (2010) 026305. doi:10.1103/PhysRevE.81.026305.
- [62] F. Olsson, J. Yström, Some properties of the upper convected maxwell model for viscoelastic fluid flow, *J. Non-Newton. Fluid Mech.* 48 (1) (1993) 125–145. doi:https://doi.org/10.1016/0377-0257(93)80068-M.
- [63] A. Lindner, P. Coussot, D. Bonn, Viscous Fingering in a Yield Stress Fluid, *Phys. Rev. Lett.* 85 (2000) 314–317. doi:10.1103/PhysRevLett.85.314.
- [64] P. Coussot, Saffman Taylor instability in yield-stress fluids, *J. Fluid Mech.* 380 (1) (1999) 363–376. doi:10.1017/S002211209800370X.
- [65] A. Eslami, S. M. Taghavi, Viscoplastic fingering in rectangular channels, *Phys. Rev. E* 102 (2020) 023105. doi:10.1103/PhysRevE.102.023105.
- [66] N. Maleki-Jirsaraei, A. Lindner, S. Rouhani, D. Bonn, Saffman–Taylor instability in yield stress fluids, *J. Condens. Matter Phys.* 17 (14) (2005) S1219. doi:10.1088/0953-8984/17/14/011.
- [67] A. P. Dufresne, T. V. Ball, N. J. Balmforth, Viscoplastic Saffman–Taylor fingers with and without wall slip, *J. Non-Newton. Fluid Mech.* 312 (2023) 104970. doi:https://doi.org/10.1016/j.jnnfm.2022.104970.
- [68] T. V. Ball, N. J. Balmforth, A. P. Dufresne, Viscoplastic fingers and fractures in a Hele-Shaw cell, *J. Non-Newton. Fluid Mech.* 289 (2021) 104492. doi:https://doi.org/10.1016/j.jnnfm.2021.104492.
- [69] M. Kawaguchi, S. Yamazaki, K. Yonekura, T. Kato, Viscous fingering instabilities in an oil in water emulsion, *Phys. Fluids* 16 (6) (2004) 1908–1914. doi:10.1063/1.1709543.
- [70] S. S. Park, D. J. Durian, Viscous and elastic fingering instabilities in foam, *Phys. Rev. Lett.* 72 (1994) 3347–3350. doi:10.1103/PhysRevLett.72.3347.
- [71] M. Constantin, M. Widom, J. A. Miranda, Mode-coupling approach to non-Newtonian Hele-Shaw flow, *Phys. Rev. E* 67 (2003) 026313. doi:10.1103/PhysRevE.67.026313.
- [72] M. Kawaguchi, Viscous Fingering of Silica Suspensions Dispersed in Polymer Fluids, *ACS Symposium Series*, 2003, Ch. 20, pp. 250–261. doi:10.1021/bk-2004-0869.ch020.

- [73] N. Kagei, D. Kanie, M. Kawaguchi, Viscous fingering in shear thickening silica suspensions, *Phys. Fluids* 17 (5) (2005) 054103. doi:10.1063/1.1894407.
- [74] D. Ozturk, M. L. Morgan, B. Sandnes, Flow-to-fracture transition and pattern formation in a discontinuous shear thickening fluid, *Commun. Phys.* 3 (1) (2020) 119.
- [75] Palak, V. R. S. Parmar, S. Chanda, R. Bandyopadhyay, Emergence of transient reverse fingers during radial displacement of a shear-thickening fluid, *Colloids Surf. A: Physicochem. Eng. Asp.* 662 (2023) 130926. doi:https://doi.org/10.1016/j.colsurfa.2023.130926.
- [76] P. Singh, S. Mondal, Viscous fingering to fracturing transition in Hele–Shaw flow of shear-thickening fluid, *Phys. Fluids* 35 (6) (2023) 064116. doi:10.1063/5.0152800.
- [77] K. Singh, M. Jung, M. Brinkmann, R. Seemann, Capillary-Dominated Fluid Displacement in Porous Media, *Annu. Rev. Fluid Mech.* 51 (1) (2019) 429–449. doi:10.1146/annurev-fluid-010518-040342.
- [78] B. Sandnes, E. Flekkøy, H. Knudsen, K. Måløy, H. See, Patterns and flow in frictional fluid dynamics, *Nat. Commun.* 2 (1) (2011) 288.
- [79] B. Sandnes, H. A. Knudsen, K. J. Måløy, E. G. Flekkøy, Labyrinth Patterns in Confined Granular-Fluid Systems, *Phys. Rev. Lett.* 99 (2007) 038001. doi:10.1103/PhysRevLett.99.038001.
- [80] F. K. Eriksen, R. Toussaint, K. J. Måløy, E. G. Flekkøy, Invasion patterns during two-phase flow in deformable porous media, *Front. Phys.* 3 (2015). doi:10.3389/fphy.2015.00081.
- [81] H. Huang, F. Zhang, P. Callahan, J. Ayoub, Granular Fingering in Fluid Injection into Dense Granular Media in a Hele-Shaw Cell, *Phys. Rev. Lett.* 108 (2012) 258001. doi:10.1103/PhysRevLett.108.258001.
- [82] C. Chevalier, A. Lindner, M. Leroux, E. Clément, Morphodynamics during air injection into a confined granular suspension, *J. Non-Newton. Fluid Mech.* 158 (1) (2009) 63–72. doi:https://doi.org/10.1016/j.jnnfm.2008.07.007.
- [83] C. Chevalier, A. Lindner, E. Clément, Destabilization of a Saffman-Taylor Fingerlike Pattern in a Granular Suspension, *Phys. Rev. Lett.* 99 (2007) 174501. doi:10.1103/PhysRevLett.99.174501.

- [84] D. Zhang, J. M. Campbell, J. A. Eriksen, E. G. Flekkøy, K. J. Måløy, C. W. MacMinn, B. Sandnes, Frictional fluid instabilities shaped by viscous forces, *Nat. Commun.* 14 (1) (2023) 3044.
- [85] X. Cheng, L. Xu, A. Patterson, H. M. Jaeger, S. R. Nagel, Towards the zero-surface-tension limit in granular fingering instability, *Nat. Phys.* 4 (3) (2008) 234–237.
- [86] S. Nand, V. Sharma, S. K. Das, S. S. Padhee, M. Mishra, Effect of Hele–Shaw cell gap on radial viscous fingering, *Scientific Reports* 12 (1) (2022) 18967. doi:10.1038/s41598-022-22769-x.
- [87] L. C. Morrow, T. J. Moronew, M. C. Dallaston, S. W. Mccue, A review of one-phase Hele-Shaw flows and a level-set method for non-standard configurations, *ANZIAM J.* 63 (3) (2021) 269–307. doi:10.1017/S144618112100033X.
- [88] A. Singh, Y. Singh, K. M. Pandey, A Review On Viscous Fingering Pattern Formation In Lifted Hele- Shaw Cell, *J. Phys. Conf. Ser.* 1455 (1) (2020) 012022. doi:10.1088/1742-6596/1455/1/012022.
- [89] T. Divoux, A. Shukla, B. Marsit, Y. Kaloga, I. Bischofberger, Criterion for Fingering Instabilities in Colloidal Gels, *Phys. Rev. Lett.* 124 (2020) 248006. doi:10.1103/PhysRevLett.124.248006.
- [90] P. H. A. Anjos, E. O. Dias, J. A. Miranda, Inertia-induced dendriticlike patterns in lifting Hele-Shaw flows, *Phys. Rev. Fluids* 2 (2017) 014003. doi:10.1103/PhysRevFluids.2.014003.
- [91] C. Gin, P. Daripa, Time-dependent injection strategies for multilayer Hele-Shaw and porous media flows, *Phys. Rev. Fluids* 6 (2021) 033901. doi:10.1103/PhysRevFluids.6.033901.
- [92] P. Singh, S. Mondal, Control and suppression of viscous fingering displacing non-Newtonian fluid with time-dependent injection strategies, *Phys. Fluids* 34 (11) (2022) 114117. doi:10.1063/5.0124066.
- [93] T. T. Al-Housseiny, P. A. Tsai, H. A. Stone, Control of interfacial instabilities using flow geometry, *Nat. Phys.* 8 (10) (2012) 747–750. doi:10.1038/nphys2396.
- [94] T. u. Islam, P. S. Gandhi, Viscous Fingering in Multiport Hele Shaw Cell for Controlled Shaping of Fluids, *Sci. Rep.* 7 (1) (2017) 16602. doi:10.1038/s41598-017-16830-3.
- [95] L. Carrillo, F. Magdaleno, J. Casademunt, J. Ortin, Experiments in a rotating Hele-Shaw cell, *Phys. Rev. E* 54 (6) (1996) 6260–6267. doi:10.1103/PhysRevE.54.6260.

- [96] T. Gao, M. Mirzadeh, P. Bai, K. M. Conforti, M. Z. Bazant, Active control of viscous fingering using electric fields, *Nat. Commun.* 10 (1) (2019) 4002. doi:10.1038/s41467-019-11939-7.
- [97] P. Li, X. Huang, Y.-P. Zhao, Active control of electro-visco-fingering in Hele-Shaw cells using Maxwell stress, *iScience* 25 (10) (2022) 105204. doi:https://doi.org/10.1016/j.isci.2022.105204.
- [98] R. Luo, Y. Chen, S. Lee, Particle-induced viscous fingering: Review and outlook, *Phys. Rev. Fluids* 3 (2018) 110502. doi:10.1103/PhysRevFluids.3.110502.
- [99] J. Kim, F. Xu, S. Lee, Formation and Destabilization of the Particle Band on the Fluid-Fluid Interface, *Phys. Rev. Lett.* 118 (2017) 074501. doi:10.1103/PhysRevLett.118.074501.
- [100] A. Kazemi, M. Norouzi, A. A. Nejad, M. Kim, K. C. Kim, S. G. Kim, An experimental study on the role and contribution of the first normal stress difference and elongational viscosity in immiscible viscoelastic saffman-taylor instability, *Chem Eng Res Des* 197 (2023) 211–227. doi:https://doi.org/10.1016/j.cherd.2023.07.036.
- [101] I. M. Coutinho, J. A. Miranda, Role of interfacial rheology on fingering instabilities in lifting Hele-Shaw flows, *Phys. Rev. E* 108 (2023) 025104. doi:10.1103/PhysRevE.108.025104.
- [102] C. A. Browne, S. S. Datta, Elastic turbulence generates anomalous flow resistance in porous media, *Sci. Adv.* 7 (45) (2021) eabj2619. doi:10.1126/sciadv.abj2619.
- [103] B. Jha, L. Cueto-Felgueroso, R. Juanes, Fluid Mixing from Viscous Fingering, *Phys. Rev. Lett.* 106 (2011) 194502. doi:10.1103/PhysRevLett.106.194502.
- [104] C. Misra, V. T. Ranganathan, R. Bandyopadhyay, Influence of medium structure on the physicochemical properties of aging colloidal dispersions investigated using the synthetic clay LAPONITE®[®], *Soft Matter* 17 (2021) 9387–9398. doi:10.1039/D1SM00987G.